Evaluation of Cleaning Methods for Multilayer Diffraction Gratings

Introduction

Multilayer dielectric (MLD) diffraction gratings are essential components for the OMEGA EP short-pulse, high-energy laser system, so they must have both high optical-diffraction efficiency and high laser-damage threshold. The cleanliness of optical surfaces intended to be deployed in high-peak-power laser systems is of paramount importance, and the fabrication of these MLD gratings involves processes that utilize a wide variety of both organic materials (photoresists, photoresist solvents, and photoresist developers) and inorganic materials (metals and oxides of various cationic elements) that may remain behind either on the surfaces or in the grooves of the MLD structure after processing. Because a substantial number of these materials can have significant optical absorbance, the incomplete removal of these residues puts the MLD gratings at an increased risk of experiencing catastrophic laser-induced damage. Although there exists a certain amount of anecdotal and empirical evidence as to the effectiveness of certain wet-chemical cleaning processes, which appear to be effective in removing trace residues from grating manufacturing, there does not exist to date a truly systematic study that strives to relate the chemical composition of contaminants introduced during the fabrication process of "structured" optical components (such as MLD gratings) with laser-induced damage. To this end, we have investigated the effectiveness of a number of wet-chemical cleaning processes currently used by the semiconductor industry for cleaning LLE-fabricated MLD gratings. The goal of this investigation was to identify a process or processes that were sufficiently aggressive in the removal of residual processing contaminants but not so aggressive as to produce physical/chemical damage to the MLD grating structure that would reduce its high diffraction efficiency.

The following chemical processes were evaluated for MLD cleaning:

Piranha Process: Piranha solution is a mixture of a strong acid (sulphuric acid, H_2SO_4) and a strong oxidizing agent (hydrogen peroxide, H_2O_2), which produces an extremely energetic solution. This composition is one of the most commonly used cleaning processes for the removal of organics (i.e., residual resist) from a surface and is usually used at a high temperature.[1,2] Although Piranha solution is highly effective in removing organic contamination, it does not remove all inorganic contaminants. Piranha solution must be prepared immediately before use, has a very limited shelf life, and cannot be stored in normal closed containers due to an explosive pressure buildup caused by the gradual loss of hydrogen peroxide gas.

Piranha + SC-1 Process: The cleaning method that is commonly used to remove inorganic contamination after Piranha clean (described above) is SC-1 (Standard Clean 1) coupled with megasonics (high-frequency ultrasonic energy).[1,3] The SC-1 solution of ammonia hydroxide, hydrogen peroxide, and DI water is also cable of removing additional organic contaminants. The megasonics aid in removing the inorganic contamination. The cavitation force generated by the megasonic frequency lifts off the contamination and also keeps these particles from re-adhering to the surface.

Hydrozone Process: Hydrozone+,[4] developed as a replacement for Piranha clean, uses ozone gas dissolved in DI water. An aqueous solution at elevated temperatures is sprayed across a surface while dry ozone gas is admitted into the cleaning chamber. The ozone diffuses through the thin boundary layer of water, in which the water hydrolyzes the organic bonds, making them susceptible to attack by O_3. The elevated water temperature maximizes the reaction rate. The reaction by-products (CO_2 and H_2O) and resist fragments are carried away in the boundary layer of water.

EKC-265[5] *and Rezi-28*[6] *Process:* These two semi-aqueous organic mixtures have been formulated as ready-to-use solutions. They contain chemistries that are effective in removing residual photoresist and post-etch and ash residues. These residue removers are formulated to be used at lower operating temperatures than standard Piranha cleans.

Nanostrip Process: Nanostrip[7] is a ready-to-use stabilized formulation of sulphuric acid (H_2SO_4) and hydrogen peroxide

(H_2O_2) compounds. This formulation was designed to remove photoresist and other organic materials at ambient temperatures and can be stored at room temperature indefinitely in closed containers without the risk of an explosive pressure buildup.

Experimental Setup

Table 108.V lists the various cleaning-process parameters evaluated for this study. Each of the processes in Table 108.V was evaluated using 100-mm-diam MLD gratings fabricated at LLE.

The grating-fabrication-process steps include (1) photoresist coated using a positive-tone resist; (2) exposure of the photoresist at 365 nm using a holographic process; (3) photoresist development; (4) reactive ion-beam etching (RIBE) of the grating pattern; (5) O_2 ion-etch clean utilizing LLE-standard-process parameters; and (6) a final wet-cleaning step. Each grating was evaluated for diffraction efficiency and laser-damage threshold both before and after the final cleaning step. All cleaned gratings were further evaluated by scanning electron microscopy (SEM), with time-of-flight secondary ion-mass spectrometry (ToF-SIMS) analysis performed on a select group of four samples.

Results

1. Diffraction Efficiency

Each cleaned MLD grating was tested for diffraction efficiency and laser-damage threshold. Pre- and post-clean diffraction efficiencies were measured across the grating using *s*-polarized light at 1054 nm with an incident beam angle of 61° (diffracted beam angle of 72°). Since there is a large variation in pre-clean diffraction efficiency, the cleaning process should increase the efficiency to our specification, but it should not decrease it to a level below our specification. Figure 108.37 shows the pre- and post-clean diffraction efficiencies for the various chemistries used. As can be observed, all of the cleaning processes meet our specification of >97% except the Piranha + SC-1. Based on SEM evidence shown later, we believe that the base SC-1 chemistry had a negative effect on the grating. The ECK-265 and Piranha-cleaned samples had the highest post-clean diffraction efficiency.

2. Laser-Damage Threshold

Laser-damage testing was conducted using 10-ps-pulsed, *s*-polarized light at 1053 nm with an incident beam angle of 61° (diffracted beam of 72°). The LLE specification for the damage threshold of our MLD gratings is 2.7 J/cm^2 at 10-ps pulse length. Figure 108.38 shows the damage-threshold values that were measured for the different cleaning processes.

The damage-threshold results indicate that only the Piranha, Nanostrip, and EKC-265 cleaning processes are capable of producing clean gratings that achieve the LLE specification.

The Nanostrip process was evaluated at different immersion times to see how this affected the laser-damage threshold. The laser-damage threshold was found to decrease with increased immersion time. This decrease in damage threshold could be due to re-deposition of organics on the surface since this work was performed in a static (un-agitated) lab-scale bath. Similarly,

Table 108.V: Process chemistries and conditions.

Process	Chemistry	Time	Temperature	Methods
Piranha	$H_2SO_4 + H_2O_2$ (various ratios)	30 min 60 min 4 h 8 h	– 60°C 90°C 110°C	Overflow bath, lab-scale beakers
Piranha + SC-1	{$H_2SO_4 + H_2O_2$ (4:1)} + {$NH_4OH + H_2O_2$ + DI (1:1:10)}	30-min Piranha + 10-min SC-1	90°C Piranha + 70°C SC-1	Overflow bath with 3-MHz megasonics
Hydrozone + (Semitool)	Di + O_3 + NH_4OH	10 min 25 min	90°C –	Single plate spray
EKC-265 (EKC Tech)	Semi-aqueous organic mixture	30 min	70°C	Overflow bath with 3-MHz megasonics
Rezi-28 (J. T. Baker)	80% aqueous base	10 min	40°C	Overflow bath
Nanostrip (Cyantek)	Stabilized formulation of $H_2SO_4 + H_2O_2$	4 h 8 h 24 h	60°C – –	Lab-scale beakers

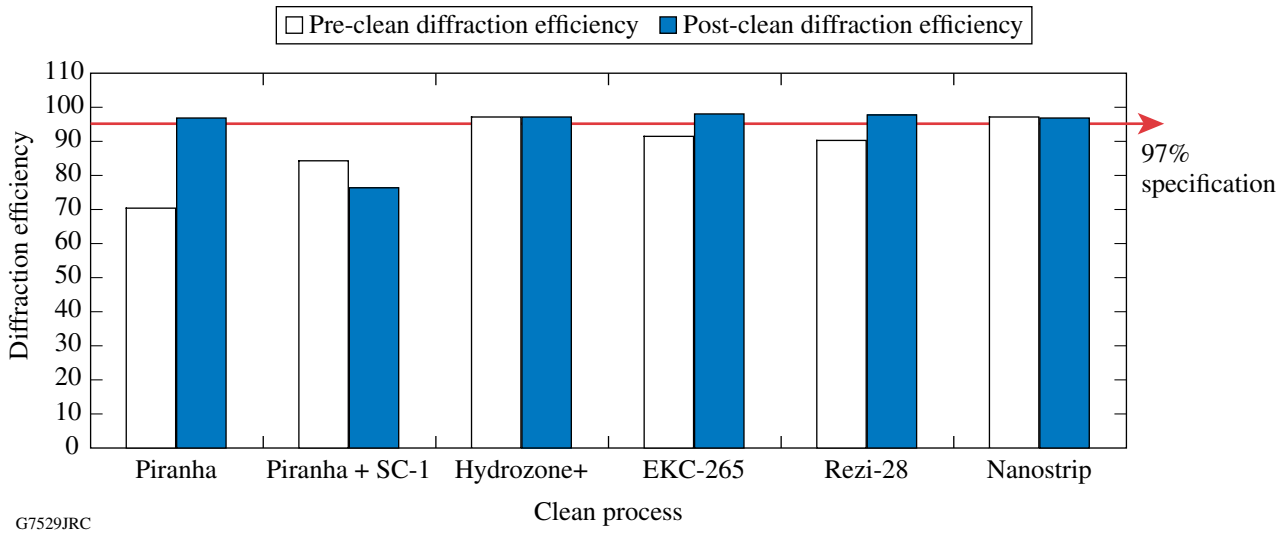

Figure 108.37
Pre- and post-clean diffraction efficiency.

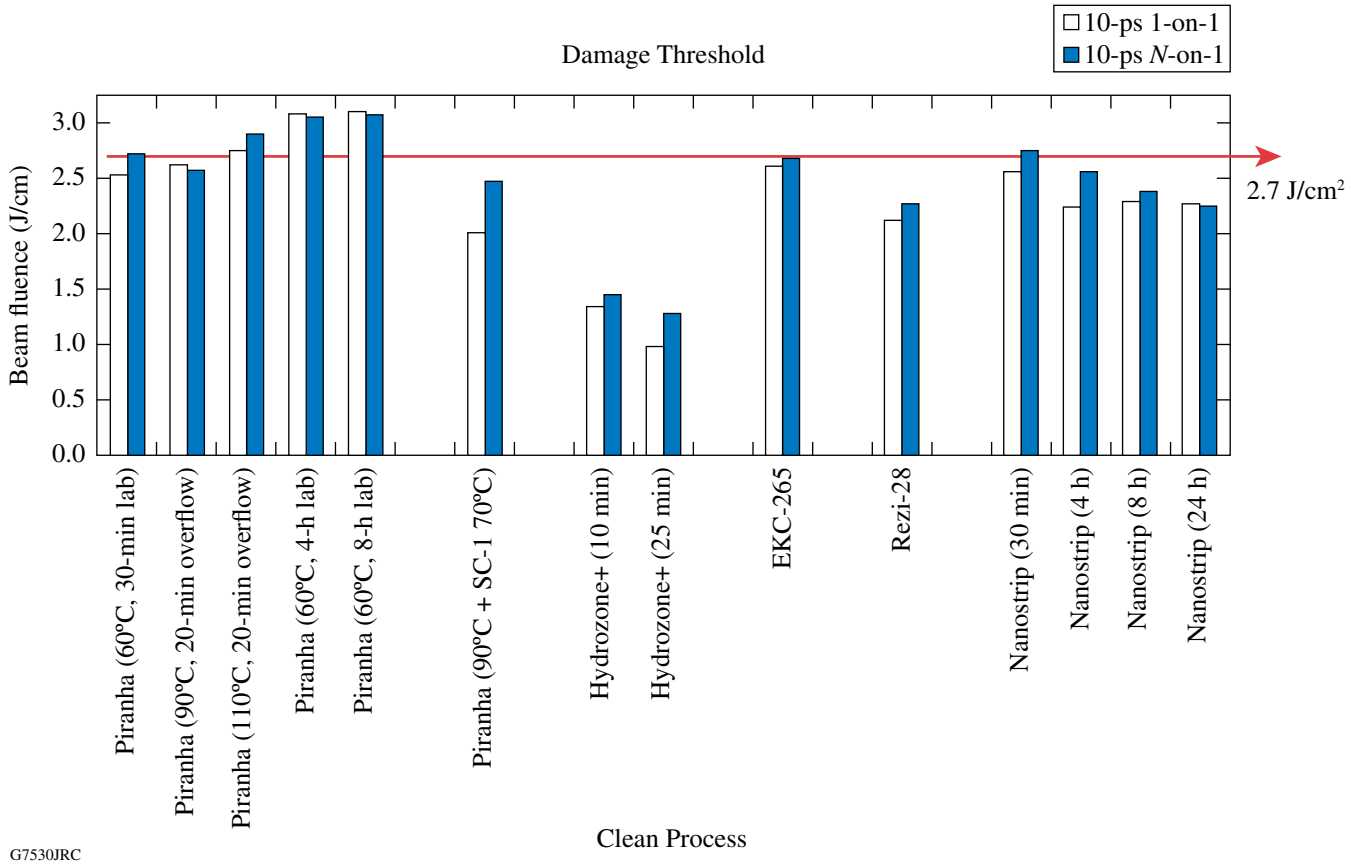

Figure 108.38
Post-clean damage threshold.

the Piranha process was evaluated at different times and temperatures. For this cleaning process, the laser-damage threshold increased as the temperature increased from 90°C and 110°C when processed in a recirculating overflow bath. Increasing the immersion time (in a static lab-scale bath) at the lower 60°C temperature also resulted in an increase in the laser-damage threshold. Additional Designs of Experiment studies are being run to fully understand reaction-rate issues of Piranha clean.

3. SEM Analysis

Scanning electron microscopy (SEM) images were collected and analyzed for each of the MLD gratings that were cleaned in this study. The SEM images of the EKC-265–cleaned and Piranha-cleaned gratings indicate there was no visual residual contamination within the grating trenches. The SEM images, along with the associated diffraction efficiency and laser-damage threshold data for these gratings, are shown in Fig. 108.39.

The SEM images along with the associated diffraction efficiency and laser-damage threshold data for the Hydrozone+, Rezi-28, and Piranha + SC-1–cleaned gratings are shown in Fig. 108.40. The Hydrozone+, Rezi-28, and Piranha + SC-1–cleaned gratings had lower laser-damage threshold values than the EKC-275– and Piranha-cleaned gratings. The Piranha + SC-1 cleaning process damaged the diffraction grating. We believe the SC-1 portion of this cleaning process, which uses a concentrated basic ammonium hydroxide solution, attacked the top amorphous SiO_2 grating layer, which caused it to decompose. Additional work is required to fully understand the failure mechanism. The Rezi-28 clean was not effective in removing the bulk photoresist from the gratings, while the Hydrozone+ clean left visual contamination within the grating trenches.

ToF-SIMS Analysis

Time-of-flight secondary ion mass spectrometry (ToF-SIMS) was performed on four different LLE diffraction-grating samples. The four samples analyzed were (1) photoresist-coated MLD (pre-clean process), (2) MLD-etched and O_2 ion-etch clean (pre-clean process), (3) Piranha-cleaned MLD, and (4) Hydrozone+-cleaned MLD.

The ToF-SIMS analysis was performed at Surface Science Western, University of Western Ontario (London, Ontario, Canada). The instrument used was an ION-TOF (GmbH), ToF-SIMS IV. A 25-keV, pulsed Bi_3^+ cluster, primary ion beam with a target current of 0.6 pA and a beam diameter of ~1.5 μm was rastered over a 500 × 500-μm^2 area on each sample. The mass range used was 10 to 1000 amu. Due to the insulating nature of the samples, a pulsed-electron flood gun was employed to neutralize charging. The analysis is sensitive to the outer one to three monolayers of the sample surface under static conditions (total primary ion dose $<10^{13}$ ions/cm^2). This technique is

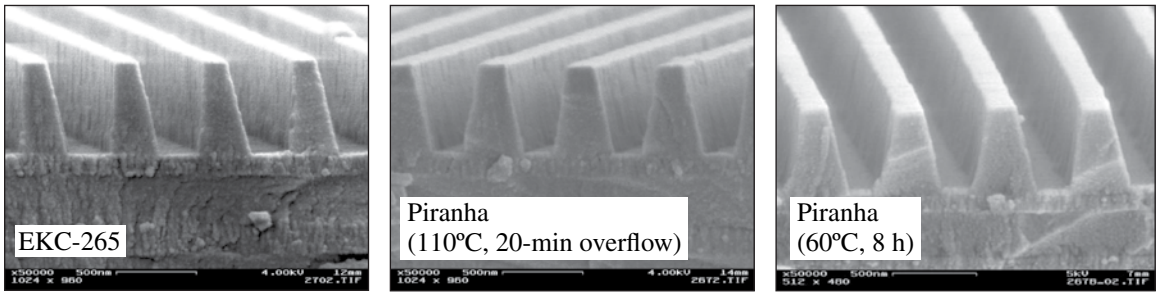

Process	Pre-clean diffraction efficiency	Post-clean diffraction efficiency	10-ps 1-on-1 (J/cm^2)	10-ps *N*-on-1 (J/cm^2)
EKC-265	91.5	98.1	2.61	2.68
Piranha (110ºC, 20-min overflow)	70.5	96.9	2.75	2.9
Piranha (60ºC, 8 h)	Not measured	Not measured	3.1	3.07

G7436JR

Figure 108.39
EKC-265 and Piranha SEM analysis with associated efficiency and damage threshold.

not absolutely quantitative; however, using peak area ratios and related normalization methods for similar substrates, meaningful and sensitive relative comparisons can be made.[8]

In order to have a numerical comparison between the samples, selected positive- and negative-ion species were chosen. Corresponding peaks were extracted and normalized to 100% (total peak areas). The normalized species are summarized in Figs. 108.41–108.43. Figure 108.41 lists species that are related to the photoresist (residual organics). This graph indicates that resist-related species remained on the surface after cleaning. The Piranha-cleaned sample had the lowest levels of resist-

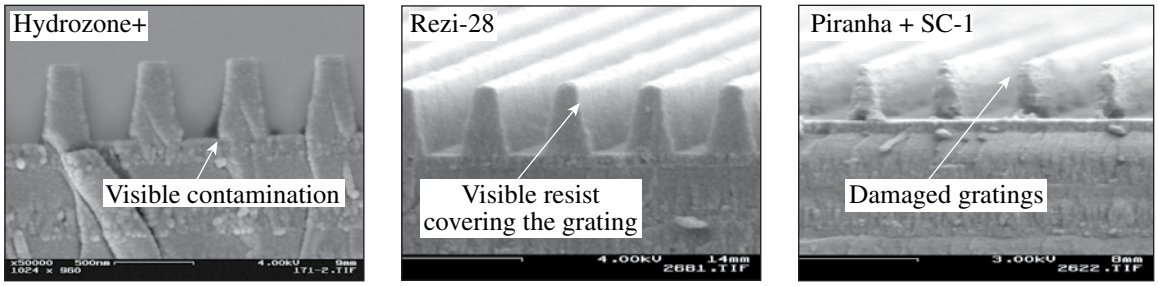

Process	Pre-clean diffraction efficiency	Post-clean diffraction efficiency	10-ps 1-on-1 (J/cm^2)	10-ps *N*-on-1 (J/cm^2)
Hydrozone+ (10 min)	97.1	97.2	1.34	1.45
Rezi-28	90.2	97.8	2.12	2.27
Piranha 110ºC + SC-1	84.2	76.4	2.01	2.47

G7435JR

Figure 108.40
Hydrozone+, Rezi-28, and Piranha + SC-1 SEM images.

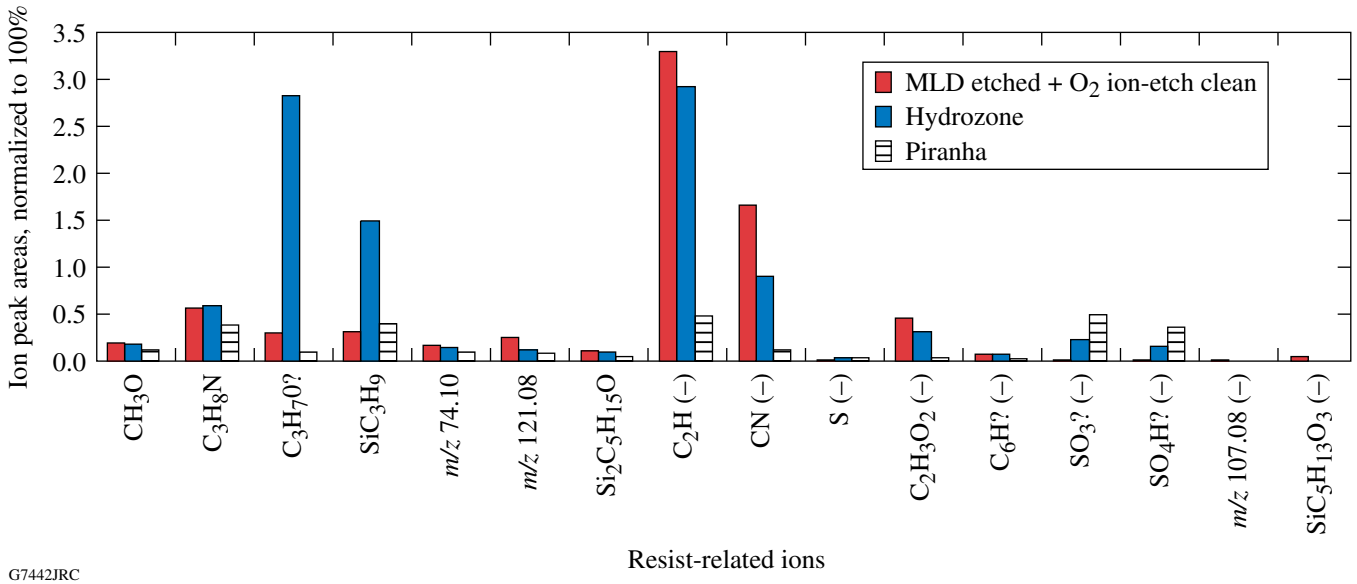

G7442JRC

Figure 108.41
Resist-related species. Note: Not all mass-to-charge (*m*/*z*) ions are able to be fully characterized. The resist sample is not shown since the level of resist-related ions approaches 100%.

related species remaining after cleaning, but there are still residual resist species that need to be removed.

The species predominantly associated with the SiO_2 grating are indicated in Fig. 108.42. Samples that have high Si-related ion peaks indicate that the surface is relatively clean since the top grating surface is SiO_2. The lack of Si-related ion peaks indicates that there were other contaminants on the surface. As shown, the Piranha and Hydrozone+ clean samples had a high signal for Si and Si_xO_y species, indicating that there is less contamination. The MLD O_2 ion-etch clean sample does not show any signal for Si or Si_xO_y species. This indicates that there was a layer of other contamination on the SiO_2 surface. The species associated with the MLD O_2 ion-etch clean sample are mainly metals, which could be originating from contamination within the etch and ash chambers (shown in Fig. 108.43). Most of these metals, however, were removed during the cleaning process.

Time-of-flight secondary ion mass spectrometry (ToF-SIMS), "shallow"-depth-profile (few tens of nanometers into the surface) scans were taken to understand the contamination of the Piranha sample. To acquire positive and negative shallow-depth profiles, a second 3-keV Cs^+ sputter ion beam was used, with a raster area of $500 \times 500\ \mu m^2$ and a target current of 12 nAS. The Bi_3^+ analysis area is centered within the sputter crater, with a raster size of $200 \times 200\ \mu m^2$. Using a raster size smaller than the sputter-crater size allows one to avoid edge effects during the depth profiling. By alternating the Bi_3^+ analysis and the Cs^+ sputter beams and

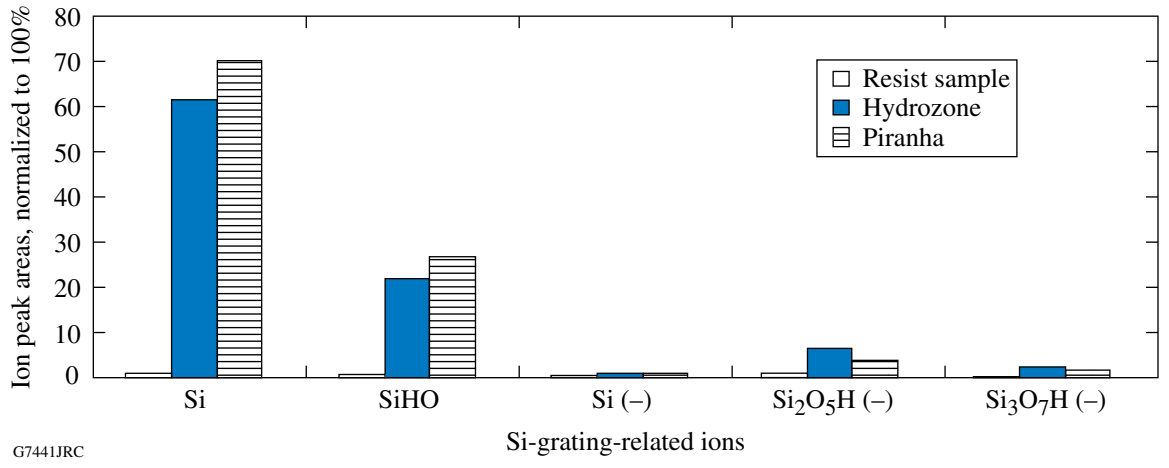

Figure 108.42
Si-related species. MLD etched + O_2 ion-etch sample does not have a Si-related signal due to other contamination covering the surface.

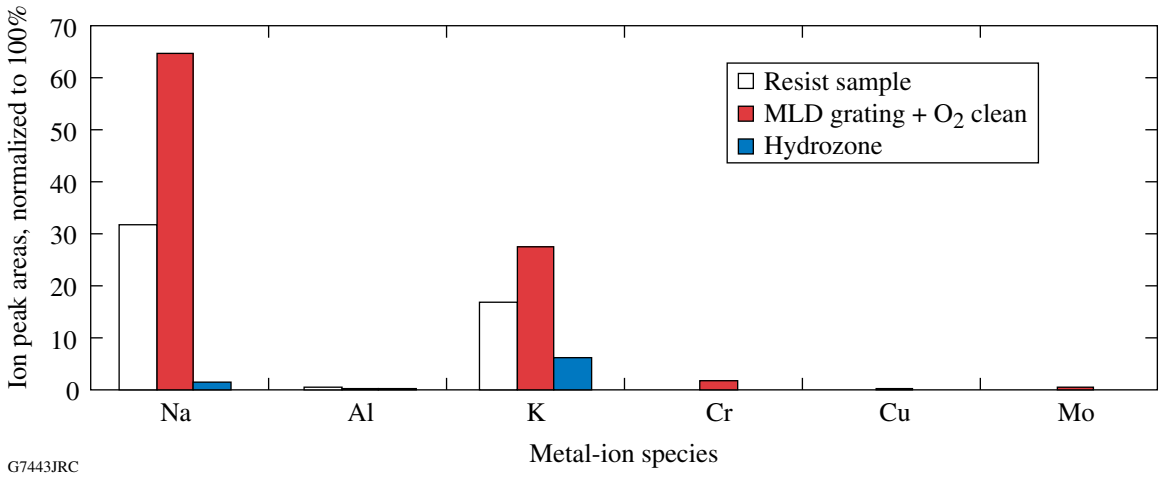

Figure 108.43
Metal-related species. Piranha-clean (not shown) process removes most metals.

inserting an electron-flood-gun pulse between for charge neutralization, a depth profile into the surface is acquired.[9]

Figure 108.44 plots the raw intensity of the positive ions detected versus the sputter time for the Piranha-cleaned sample. This sample yields various ions with Si^+ being the dominant one. Directly at the grating surface there was an abundance of Si^+ (silicon ion), $SiOH^+$ (silicon hydroxide ion), K^+ (potassium ion), O^+ (oxygen ion), Na^+ (sodium ion), Cr^+ (chromium ion), Fe^+ (iron ion), and Al^+ (aluminum ion). As the analysis probed deeper into the SiO_2 surface, additional major ions detected were Si^+, K^+, $SiOH^+$, O^+, Na^+, Fe^+, and Al^+. The Si^+ and $SiOH^+$ ions were from the SiO_2 grating, as one would expect. The oxygen originated from the etch process and was being "implanted" into the SiO_2 grating surface during the reactive ion-beam etch (RIBE). The metals Cr^+, Fe^+, and Al^+ originated from the etch chamber and became implanted into the SiO_2 grating surface. The potassium and sodium ions were surmised to come from multiple contamination sources. Some of the possible sources of this contamination could have been the rinse water, developer, materials used during cleaning (beakers), and general handling. Additional tests need to be done to better understand this contamination.

The concentration of negative-ion species detected versus sputter time is plotted in Fig. 108.45. The major ions detected were O^- (oxygen ion), SiO_2^- (silicon oxide), F^- (fluorine ion), Si^- (silicon ion), SO_3^- (sulfate ion), Cl^- (chlorine ion), CN^- (cyanide ion), C_2H^- (carbon ion), and C^- (carbon ion). The oxygen, fluorine, chorine, and carbon ions were implanted from the etch process and chamber. The silicon-related ions originated from the silicon oxide grating, while the sulfate ion originated from the sulfuric acid–cleaning process.

Conclusions

Using 100-mm-diam MLD gratings fabricated at LLE, we evaluated different cleaning methods designed to optimize both optical diffraction efficiency and laser-damage threshold of these gratings for the OMEGA EP Laser System. Pre- and post-clean diffraction efficiency and laser-damage threshold were measured for each of the samples. Scanning electron microscopy (SEM) images were collected and analyzed to understand if any visual surface contamination existed after cleaning. Additionally, a baseline time-of-flight secondary ion-mass spectrometry (ToF-SIMS) and shallow-depth profile analysis was performed to understand the type of contamination remaining after the different process steps.

The diffraction efficiency, laser-damage threshold, and SEM images all show that the Piranha clean merits further exploration. The MLD gratings cleaned by the Piranha processes had the highest diffraction efficiency and laser-damage-threshold

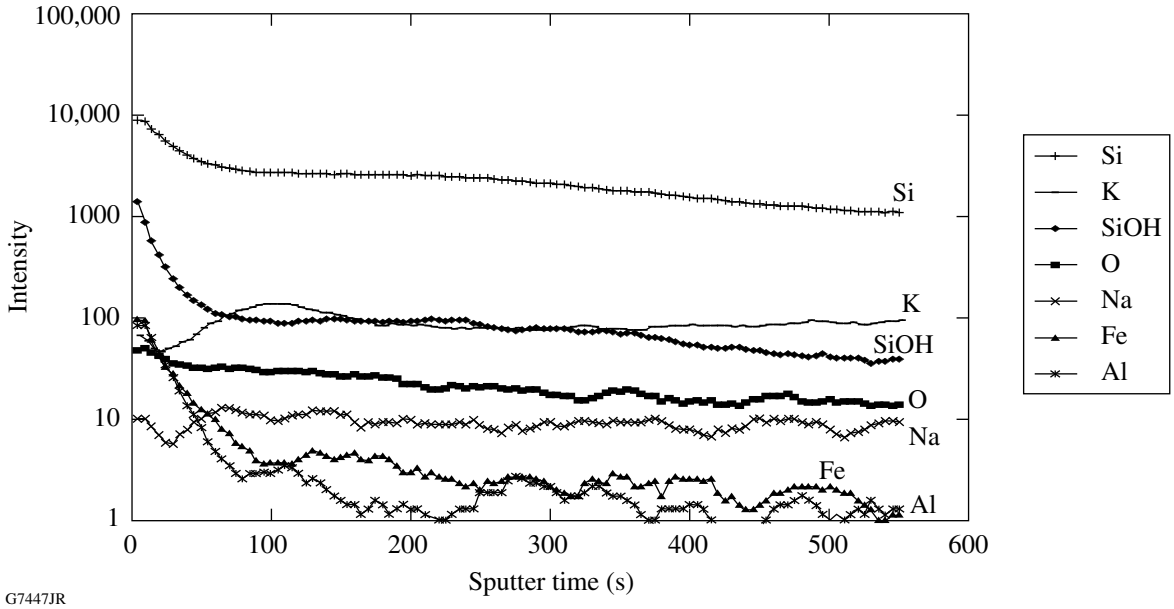

Figure 108.44
Piranha-clean positive-ion depth profile.

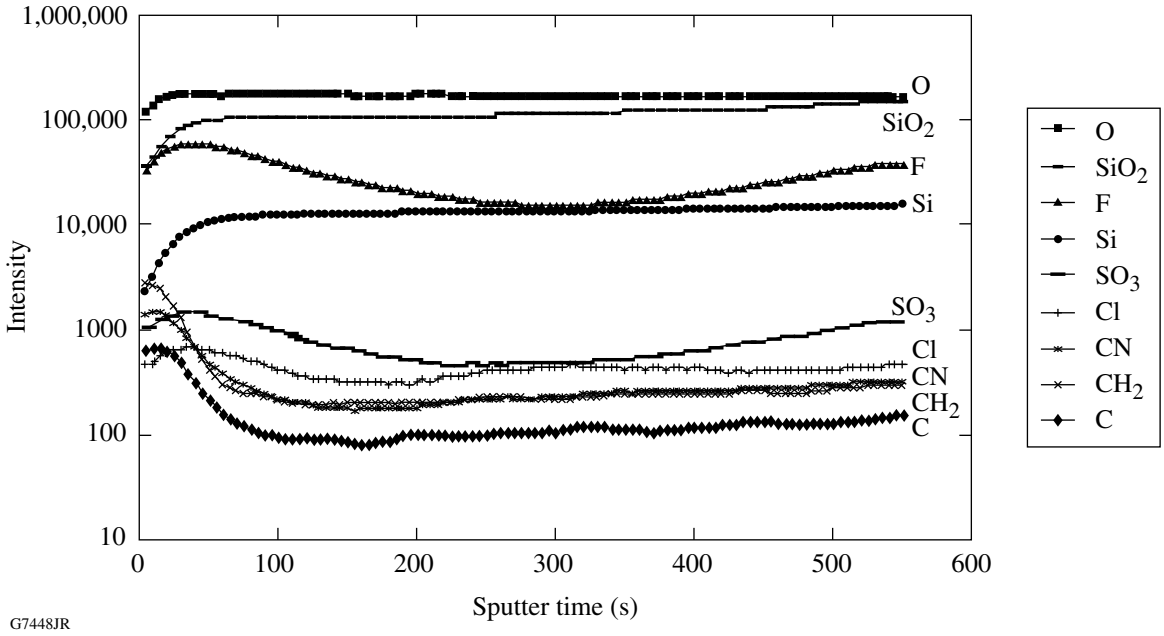

Figure 108.45
Piranha-clean negative-ion depth profile.

values. The SEM images also validated these results by showing no visual contamination after cleaning.

ToF-SIMS analysis was performed on four types of samples from the LLE grating project to acquire a baseline for surface residual contamination. The encouraging results show that the cleaning process can remove a large portion of the photoresist (organic) contamination even without optimization of cleaning-process variables. It was further found that there is a monolayer of contamination (mostly metal ions) after etch and O_2 ion-etch clean processing. The shallow-depth profile analysis provides an understanding of the contaminants implanted in the grating surface, which in turn allows identification of the source of most of the ions detected. Understanding the sources and depth of "implantation" of these ions will assist LLE in developing an optimized grating-cleaning process. Further Design of Experiment studies will be evaluated to understand the interaction of the variables within the cleaning process. LLE will continue to use SEM and ToF-SIMS analysis to characterize the surface after each cleaning test.

ACKNOWLEDGMENT

This work was supported by the U.S. Department of Energy Office of Inertial Confinement Fusion under Cooperative Agreement No. DE-FC52-92SF19460, the University of Rochester, and the New York State Energy Research and Development Authority. The support of DOE does not constitute an endorsement by DOE of the views expressed in this article.

REFERENCES

1. W. Kern, *Handbook of Semiconductor Wafer Cleaning Technology: Science, Technology, and Applications*, Materials Science and Process Technology Series (Noyes Publications, Park Ridge, NJ, 1993), pp. 3–56.

2. S. Clark, Bold Technologies, Inc., West Jordan, UT 84088, http://www.bold-tech.com/technical/piranha_etch.html (2000).

3. R. S. Ridley, Sr. et al., in *1998 IEEE/SEMI Advanced Semiconductor Manufacturing Conference* (IEEE, Boston, 1998), pp. 235–242.

4. Semitool, Kalispell, MT 59901.

5. EKC265 product sheet, EKC Technology, Inc., Hayward, CA 94545, November 2006, http://www2.dupont.com (6 November 2006).

6. Rezi-28 product sheet, Mallinckrodt Baker, Inc., Phillipsburg, NJ 08865, November 2006, http://www.mallbaker.com (11 November 2006).

7. NANO-STRIP™ product sheet, Cyantek Corporation, Fremont, CA 94539-5652, http://www.cyantek.com (2006).

8. Dr. James Francis, ToF-SIMS Results, Surface Science Western, email reports and private communication (6 April 2006).

9. Dr. James Francis, ToF-SIMS Report, Surface Science Western, email reports and private communication (9 August 2006).